Observation of the long-term variability of Cygnus X-1 with MAXI

Juri Sugimoto,[1,2] Shunji Kitamoto,[2] Tatehiro Mihara[1] and the MAXI team

[1] MAXI team, Institute of Physical and Chemical Research (RIKEN), 2-1 Hirosawa, Wako, Saitama 351-0198, Japan
[2] Department of Physics, Rikkyo University, 3-34-1 Nishi-Ikebukuro, Toshima, Tokyo 171-8501, Japan
E-mail(JS): sugimoto@crab.riken.jp

ABSTRACT

We studied the long-term X-ray variability of the black hole binary, Cygnus X-1, using about 6 years of MAXI data from 2009 to 2016, in the high/soft state (HSS) and the low/hard state (LHS). We analyzed an aperiodic long-term variation, using Normalized Power Spectrum Densities (NPSDs), in the frequency range from 10^{-7} to 10^{-4} Hz, with $2-4$ keV, $4-10$ keV and $10-20$ keV data. From the comparison with previous works in the frequency region above 10^{-3} Hz, it was shown that the NPSD extends with a single index from 10^{-3} to 10^{-7} Hz in both the LHS and HSS. Such the long-term variation is mostly caused by the power-law component in the energy spectrum. In the LHS, the variability slightly decreased towards higher energies, while in the HSS, the variability was found to increase significantly with energy. To explain our results of the long-term aperiodic variation, we propose a new large-scale disk structure. In our model, an optically-thin and geometrically-thick accretion flow coexists with an optically-thick and geometrically-thin, standard accretion disk, which is extending up to a large radius of $\sim 10^{12}$ cm, in both HSS and LHS.

KEY WORDS: black hole physics — accretion, accretion disks—X-ray:general — stars: individual: Cygnus X-1

1. Introduction

In the X-ray universe, a mass accretion is seen in various phenomena. Among them an accretion disk is commonly formed around a compact star in an X-ray binary system. Such a compact star shines releasing the gravitational energy of the accreting gas from the companion star. The X-ray binary, especially with a black hole (BH), is studied by a lot of researchers, focusing on the accretion disk, including the accretion flow.

An important information obtained from observations is a time variation of the X-ray intensity. In fact, the typical BH binary, Cygnus X-1 (Cyg X-1), is drawn attention to its violent time-variation since its discovery in 1960's. It has an irregular and large-amplitude variation in the range of $0.1 \sim$ a few second. The cause of the time variation is related with the characteristics of the accretion flow in the accretion disk, especially within $10\,r_{\rm S}$ ($r_{\rm S}$ is the Schwarzschild radius) where majority of X-rays are emitted.

On the other hand, the long-term variation more than 1000 s is not well understood. Because most of observations are made by X-ray telescopes mounted on the satellites orbiting a low Earth orbit. Such a time variation in the scale of several tens of days is important to understand the complete structure of the accretion disk. In order to investigate the over all structure of the accretion disk, especially of Cyg X-1, we studied aperiodic long-term variation of the intensity. We use the X-ray data obtained by MAXI which provides us a statistically good X-ray intensity and a spectrum every 90-minite spaning more than six years.

2. Observation

We analyzed the data of Cyg X-1 obtained with MAXI (Matsuoka et al. 2009). We downloaded archival data of Cyg X-1 of one-day bin and 90-

minute bin from the MAXI home page[1].

Figure 1 showed one-day bin light curves of Cyg X-1 obtained with the GSC from 2009 August 15 (MJD = 55058) to 2016 January 30 (MJD = 57417), in three energy bands ($2-4$ keV, $4-10$ keV and $10-20$ keV). A time history of the hardness ratio (HR), $I(4-10$ keV) / $I(2-4$ keV), is also plotted. The state of Cyg X-1 can be recognized by the values of the HR as the HSS (HR$<$0.43) and the LHS (HR$>$0.48).

Since the start of the MAXI observation in 2009 August, Cyg X-1 was in the LHS for about ten months. At around MJD = 55378, the source made a transition to the HSS, where it stayed for another ten months. After several times of state transitions, it has been mainly in the HSS since MJD = 56078.

3. Analysis

3.1. Definition of NPSDs

The X-ray light curve with 90-minute bin was converted to the PSD by the discrete Fourier transformation as,

$$F_{\rm c}(f) = \frac{2}{N}\sum_{j=1}^{N} y_j \cos(2\pi f \Delta t \times j),$$

$$F_{\rm s}(f) = \frac{2}{N}\sum_{j=1}^{N} y_j \sin(2\pi f \Delta t \times j), \quad (1)$$

where y_i is the intensity (photons s^{-1} cm^{-2}) at the i-th bin, N is the number of data after filling the gaps as described in Sugimoto et al. (2016), and Δt is a time interval of 5400 s, which is the regular sampling time of the MAXI public data, f is the frequency which is an integer multiple of Δf=$\frac{1}{T}$ and T is the total time span of the observation. The factor of $2/N$ is employed so that $F_c(f)$ and $F_s(f)$ represent the amplitude of the cosine and sine components, respectively, regardless of N. The power, $\frac{1}{2}(F_{\rm c}^2(f)+F_{\rm s}^2(f))$, is that in the frequency range Δf. Therefore the PSD, power per Hz, is,

$$P(f) = \frac{1}{2\Delta f}\left\{F_{\rm c}^2(f)+F_{\rm s}^2(f)\right\}. \quad (2)$$

The unit is (RMS^2/Hz). To represent relative amplitude, the PSD is normalized by the square of the average intensity following Miyamoto et al. (1994). It is called an Normalized PSD (NPSD).

To obtain the real NPSD from the MAXI data two corrections are necessary; the gap correction and the aliasing correction. The MAXI data are not completely regular-sampled. Sometimes data gaps are caused by sun avoidance, high particle background regions, small dead regions around the scan poles which move with the precession period of the orbit of the ISS, and other effects. Furthermore, MAXI measurements are snapshots. It scans an X-ray source only for $40 \sim 70$ s, every 5400 s period. Each data point is a very short snapshot, with a long interval to the next sampling. As a result, a MAXI data point contains source variations not only on time scale longer than 5400 s, but also to these in between $40 \sim 70$ s and ~ 5400 s. We described the estimation of these effects and derived a "transfer function" for the calculated PSD to the best estimation of the real PSD in Sugimoto et al. (2016).

3.2. Long-term PSDs v.s. short-term PSDs

Although we can make a long-term PSD by using all the 6years of data, single PSD is difficult to estimate the errors of data points. We shorten the data length to 40 and 43 days for the LHS and the HSS, respectively, calculated NPSDs, and averaged them. The errors of NPSDs obtained in this way can be expected statistically and have smaller errors. Instead, it lacks the information in the lowest frequencies. The data span covers a frequency range down to $\sim 3\times10^{-7}$ Hz. Six data segments were extracted for the LHS, and eight data segments for the HSS. Then, we converted these data segments individually into NPSDs, and took their averages over the LHS and HSS separately.

Figure 2 shows our $4-10$ keV NPSDs in both states, in comparison with previous works with RXTE data by Cui et al. (1997), Pottschmidt et al. (2003), and Reig et al. (2002). In both states, our results at 10^{-4} Hz locate on simple extrapolations of the NPSDs obtained previously by the RXTE/PCA in the frequency region above 10^{-3} Hz. The NPSD in Reig et al. (2002), which is obtained by the RXTE/ASM, is located between the two states of the present work. This difference is presumably because their data included some of the HSS and the transition periods, although the main part was in the LHS.

[1] http://maxi.riken.jp/top/index.php?cid=1&jname=J1958+352

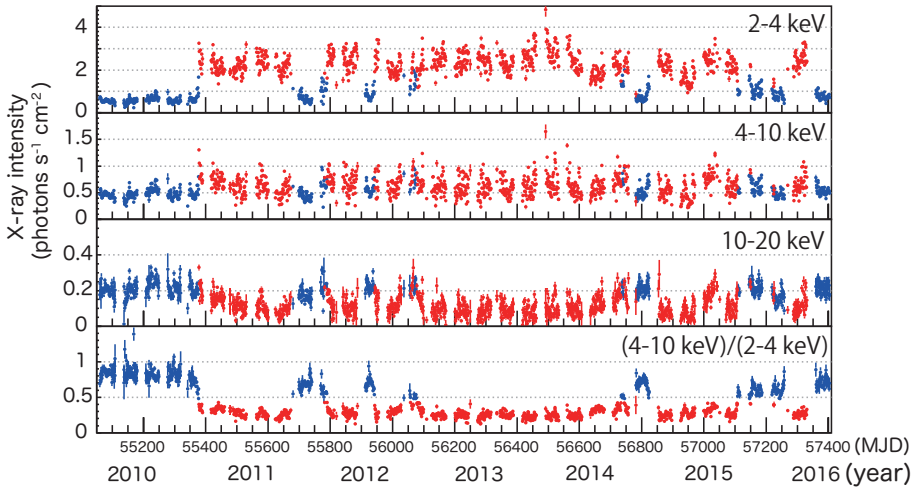

Fig. 1. One-day bin light curves and HR histories of Cyg X-1 obtained with the MAXI/GSC. From the top to bottom panels, the $2-4$ keV, $4-10$ keV and $10-20$ keV intensities, and the hardness ratio, $I(4-10\,\mathrm{keV})$ / $I(2-4\,\mathrm{keV})$, are plotted. The blue and red regions indicate the LHS and the HSS periods, respectively. Data points with large error bars, due to high background counts, were omitted.

3.3. Energy dependence of the long-term NPSD in the HSS

The long-term NPSD in the HSS was obtained for the first time. Figure 3 shows the NPSD in the HSS in the frequency range of 3 hours to 1 month. The vertical error bars represent the NPSD scattering (standard deviation) within each ensemble. We found that the high-energy bands ($4-10$ keV and $10-20$ keV), which correspond to the power law component in the energy spectrum, are more variable than the low energy band ($2-4$ keV), which corresponds to the disk component. It means that the power law component is responsible for the observed long-term intensity variations, while the disk emission is essentially constant.

4. Discussion

The short-term variation above 10^{-3} Hz is thought to reflect the phenomena occurring in the vicinity of the BH. On the other hand, it is unlikely that the long-term variation in the range of 10^{-7} Hz is generated there. We consider that it is generated at a large radius and propagates inwards as a variation of the mass accretion rate. Then most of the X-rays are radiated from the vicinity of the BH. Here, we discuss that how the long-term variation is propagated to the vicinity of the BH. The time scales of the variation newly produced in the accretion disk are the dynamical time scale, $t_{\rm d}$, and thermal time scale, $t_{\rm th}$, expressed as

$$t_{\rm d} = \Omega_{\rm K}^{-1}, \qquad t_{\rm th} = (\alpha\Omega_{\rm K})^{-1}. \tag{3}$$

On the other hand, the time scale of the accretion is the viscous time scale of the accretion disk, $t_{\rm vis}$, expressed as

$$t_{\rm vis} = (\alpha\Omega_{\rm K})^{-1}\left(\frac{H}{r}\right)^{-2}. \tag{4}$$

We compared these time scales in the standard disk and in the RIAF. In an optically-thick and geometrically-thin standard disk, the thickness of the disk H is much smaller than the radius r. Then, the viscous time scale is larger than the other two time scales, and variations produced at any outer radii would be strongly dissipated and would not propagate down to the X-ray emitting region. On the other hand, in an optically-thin and geometrically-thick flow (RIAF), H is the same level as r. In this case the thermal time scale is of the same order as the viscous time scale, and the fluctuations can propagate inwards, varying the X-ray intensity on a wide range of time scales.

Then, we proposed a new large-scale accretion disk structure as illustrated in figure 4. The optically-thin flow (RIAF) should co-exist from the vicinity of the BH to the radius of $\sim 10^{12}$ cm.

The long-term variation produced at the large radius is transported to the vicinity of the compact star, via the RIAF, and eventually X-ray intensity of the power law component shows the long-term variation.

5. Conclusion

Using six years archival data obtained with MAXI, we derived the NPSDs of Cyg X-1 in its LHS and HSS from 10^{-7} Hz to 10^{-4} Hz in the three energy bands. It is paticularly important that the long-term variations in the two states were studied in a unified way using the same instrument, with the same analysis method, and under similar data statistics. The PSD of the both states in the frequency range between 10^{-5} and 10^{-4} Hz were also provided by our work for the first time. Our results in both states were approximated by a power law, and on an extrapolation of the NPSD previously obtained in frequencies above 10^{-4} Hz.

Also the long-term NPSD in the HSS was obtained for the first time. The NPSD from 10^{-7} Hz to 10^{-4} Hz in the HSS depends on energy in such a way that it is 5∼6 times higher in the $10 - 20$ keV band than that in the low energy band ($2 - 4$ keV). This result is expected to provide some clues to the still unknown origin of the hard-tail component, which is nearly always observed in the HSS.

We then proposed a new disk structure. The optically-thin corona should extend to $\sim 10^{12}$ cm, and a standard optically-thick and geometrically-thin disk co-exists in the out side of the certain radius. The long-term variation produced at the large radius is transported to the vicinity of the compact star, via the optically-thin corona, and eventually X-ray intensity of the power law component shows the long-term variation.

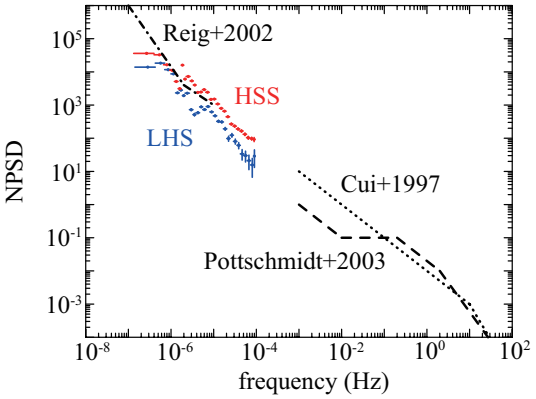

Fig. 2. A comparison of the MAXI $4 - 10$ keV NPSDs in the LHS (blue) and the HSS (red), with the previous works. The dashed line is the $2 - 13$ keV NPSD in the LHS by Pottschmidt et al. (2003), the dotted line is that in the HSS in $2 - 13$ keV by Cui et al. (1997), and the dot-dashed line is that by Reig et al. (2002), where the most data are in the LHS.

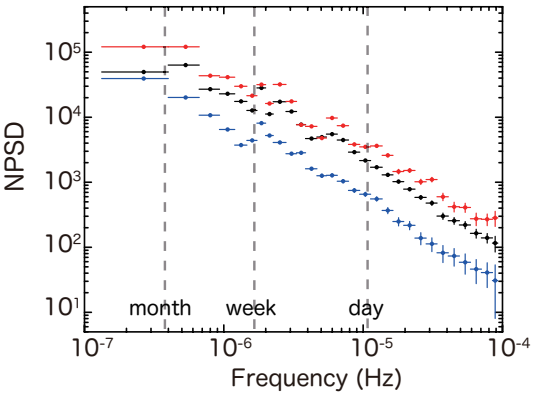

Fig. 3. The NPSDs calculated over data segments (43 d × 8 for the HSS), and averaged.

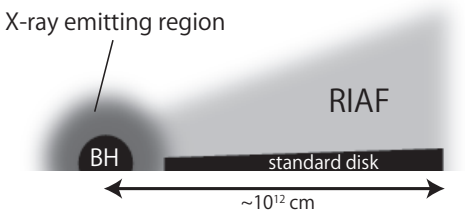

Fig. 4. Illustration of our accretion model.

References

Churazov, E. et al. 2001, *MNRAS.*, 321, 759
Cui, W. et al. 1997, Transparent Universe, 382, 209
Matsuoka, M. et al. 2009, *PASJ*, 61, 999
Mihara, T. et al. 2011, *PASJ*, 63, 623
Miyamoto, S. et al. 1994, *ApJ*, 435, 398
Pottschmidt, K. et al. 2003, *A&A*, 407, 1039
Reig, P. et al. 2002, *A&A*, 383, 202
Sugimoto, J. et al. 2016, *PASJ*, 68, S17
Tomida, H. et al. 2011, *PASJ*, 63, 397